

# Mutual Calibration of a Camera and a Laser Rangefinder

Vincenzo Caglioti, Alessandro Giusti and Davide Migliore

Politecnico di Milano, Dipartimento di Elettronica e Informazione, Italy

**Abstract.** We present a novel geometrical method for mutually calibrating a camera and a laser rangefinder by exploiting the image of the laser dot in relation to the rangefinder reading.

Our method simultaneously estimates all intrinsic parameters of a pinhole natural camera, its position and orientation w.r.t. the rangefinder axis, and four parameters of a very generic rangefinder model with one rotational degree of freedom. The calibration technique uses data from at least 5 different rangefinder rotations: for each rotation, at least 3 different observations of the laser dot and the respective rangefinder reading are needed. Data collection is simply performed by generically moving the rangefinder-camera system, and does not require any calibration target, nor any knowledge of environment or motion.

We investigate the theoretical limits of the technique as well as its practical application; we also show extensions to using more data than strictly necessary or exploit a priori knowledge of some parameters.

## 1 Introduction

We consider a rangefinder-camera system and a solidal frame of reference  $F$ ; the rangefinder itself can rotate around a generic axis solidal to  $F$ . After the mutual calibration is completed, we can:

- recover the viewing ray (in the reference frame  $F$ ) associated to any image point (camera calibration);
- recover the measuring ray (in the reference frame  $F$ ) associated to any rangefinder angle, and a point on this ray which returns a zero reading (rangefinder calibration).

Mutual rangefinder-camera calibration is needed for relating rangefinder readings to the respective image points; this is a prerequisite for correlating rangefinder and image data, which is useful for many practical tasks such as obstacle detection and characterization, 3D shape and texture reconstruction, robot self-localization, odometry and mapping. Our proposed solution does not require any specific calibration object, and can be performed automatically by just sampling rangefinder readings and camera images during generic relative motion of the rangefinder-camera system or the surrounding scene: the only requirement is that you get at least three different range readings for each of five different rangefinder angles.

The problem is hard since it is characterized by many variables and degrees of freedom, related to the camera characteristics, camera position, and rangefinder construction. In its most general form, the problem assumes almost no knowledge on the system characteristics and environment parameters; on the other hand, each of our observations is very basic and it only consists in a point on the image and the related rangefinder reading. When compared to the problem of calibrating a camera alone without any prior knowledge of the environment (autocalibration), our technique is surprising for its simplicity, especially if accounting for the additional degrees of freedom which characterize this scenario. This is intuitively explained by considering that our technique exploits some properties of the rangefinder function (such as the linearity of the measuring ray): therefore, while being calibrated, it also provides constraints for camera calibration, and vice-versa. An interesting related work from this point of view is [8], which calibrates a camera using a laser pointer as a calibration device.

Our work heavily relies on known techniques in projective geometry [5]. In particular, our camera calibration technique is related to the method introduced by Colombo *et al.* in [2], which calibrates a camera using coaxial circles; other interesting algebraic properties of coplanar circles for camera calibration and 3D structure extraction are presented in [4, 6]. The problem of simultaneously calibrating a camera and a laser rangefinder has been recently challenged with several approaches: in [9], a checkerboard calibration pattern is used, and its images and distance profiles are related in order to find the camera position and orientation w.r.t. the rangefinder; in [1] a special 3D calibration object allows to automatically calibrate a laser rangefinder. Our technique is different in that it does not use any explicit calibration target, but exploits the visible image of the laser dot; a similar approach is found in [7], where some algebraic constraints on the camera-rangefinder calibration due to the laser dot visibility are derived.

In Section 2 we formally define the problem and its parameters and variables. Section 3 presents our technique, and sketches the extension to 2-DOF rangefinders. Section 4 discusses the results, and proposes variations for calibrating only a subset of the parameters, and using more data than strictly needed.

## 2 Definitions, Model and Data

### 2.1 System Model

We consider a camera-rangefinder system; the rangefinder has 1 rotational DOF around a generic axis; the rangefinder rotation angle  $\phi$  is not calibrated – i.e., the actual angle is not necessarily known, but repeatable.

We define a reference frame  $F$  as follows:

- $F_z$  coincides with the rangefinder rotation axis;
- $F_x$  is parallel to the projection on the  $xy$  plane of the rangefinder ray when  $\phi = 0$ ;
- the origin is placed at the nearest point on the rotation axis to any telemeter ray.

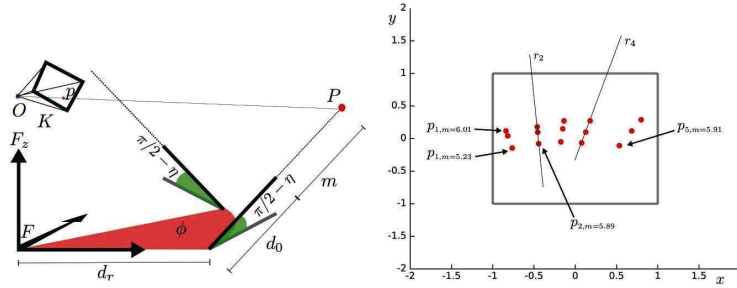


**Fig. 1.** Left: geometrical model of the system. Right: the minimal number of observations. For each of the observed laser dots, the corresponding rangefinder measure is known. At least three points are needed for each of 5 rangefinder angles.

## 2.2 System Parameters

Let  $r$  be a generic rangefinder ray; the rangefinder parameters are the following:

- the distance  $d_r$  between  $r$  and  $F_z$ ;
- the angle  $\eta$  between  $r$  and  $F_z$ ;
- the distance  $d_0$  between the point on  $r$  originating a zero rangefinder reading and the point on  $r$  nearest to  $F_z$ .

The camera parameters are expressed by the familiar perspective camera calibration matrix  $P$ . More specifically, the intrinsic parameters are summarized by the  $K$  matrix, on which we assume null skew factor, resulting in 4 degrees of freedom: aspect ratio  $a$ , focal length  $f$ , and the principal point coordinates  $u_0, v_0$ . By considering 6 additional degrees of freedom for the camera generic position and rotation w.r.t.  $F$ , the camera model is characterized by 10 degrees of freedom.

In total, we are going to estimate a total of 13 system parameters.

## 2.3 Observation Model

The calibration procedure is based on a set of observations. Each observation  $o$  is characterized by:

- a rangefinder rotation angle  $\phi$ , not necessarily calibrated but repeatable;
- a rangefinder reading  $m$ ;
- an image point  $p = (u, v)$ , where the laser dot is observed.

We assume that the rangefinder reading is linear w.r.t. the actual distance in the scene, up to the constant additive factor modeled by the rangefinder parameter  $d_0$ .

$\phi$  and  $m$  identify a point in space, therefore they uniquely define the image point  $p$  through the camera calibration matrix  $P$  and the rangefinder parameters.

### 3 Calibration Procedure

#### 3.1 Data Gathering

Our calibration procedure uses at least 15 observations; in Section 4 we show how the procedure is extended in order to take advantage of additional observations or parameters known *a priori*.

We consider 5 different  $\phi$  angles  $\phi_i$   $i = 1..5$ . For each  $i$ , we need 3 observations  $o_{i,j}$   $j = 1..3$  characterized by different  $m$  values. These observations can be easily automatically gathered by simply moving the camera-rangefinder system in an environment, or by moving large objects in front of the still system.

$$o_{i,j} = \{i, m_{i,j}, p_{i,j}\} \quad (1)$$

#### 3.2 Recovering Images of Coaxial Circles

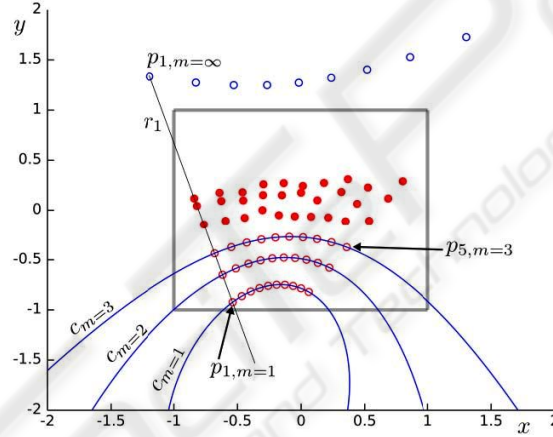


**Fig. 2.** Three conics can be recovered by exploiting the cross ratio invariance under perspective transformations. Note that in this figure, observations for more than 5 angles are depicted.

$p_{i,1}, p_{i,2}, p_{i,3}$  are image points all lying on the same image line  $r_i$  because they are projections of scene points  $P_{i,1}, P_{i,2}, P_{i,3}$  (the laser dots) lying on the same scene line, i.e. the rangefinder ray  $R_i$ <sup>1</sup>. The distances between scene points  $P_{i,1..3}$  are known from the respective rangefinder readings  $m_{i,1..3}$ : therefore, by exploiting the cross ratio invariance under a perspective transformation, any point on image line  $r_i$  can be associated to the related rangefinder reading.

Let  $p_{i,m=x}$  be the image point projection of the laser dot associated to rangefinder reading  $x$ . We can now retrieve  $p_{i,m=x}$  for any  $x$ . Then we compute  $p_{i,m=1}, p_{i,m=2}$  and  $p_{i,m=3}$ .

<sup>1</sup> Even if the camera-rangefinder system is moved for gathering the observations, we are currently considering reference frame  $F$ , which is solidal with the system itself

The procedure can be repeated for all of the 5 angles  $\phi_i$   $i = 1..5$ . As a result, we get another set of 15 points, corresponding to the projections of the laser dots associated to the rangefinder readings  $m = 1$ ,  $m = 2$  and  $m = 3$  for each of the 5  $\phi_i$  angles. Note that some of these image points may lie outside the imaged part of the image plane.

The 5 image points  $p_{i,m=x}$  (with  $i = 1..5$ ) all lie on a conic  $c_{m=x}$ , because they are projections of scene points lying on a circumference  $C_{m=x}$  in the scene. The axis of  $C_{m=x}$  is the rangefinder rotation axis  $F_z$ . We can reconstruct  $c_{m=1}$ ,  $c_{m=2}$  and  $c_{m=3}$  as we have 5 points belonging to each.

### 3.3 Computing the Camera Intrinsic Parameters

The images  $c_{m=1}$ ,  $c_{m=2}$  and  $c_{m=3}$  of three coaxial circles allow to calibrate the camera parameters, and to recover the camera position with respect to the rangefinder. The first step is to exploit  $c_{m=1}$ ,  $c_{m=2}$  and  $c_{m=3}$  in order to identify some vanishing points representing orthogonal directions; then, the intrinsic camera parameters are determined by exploiting the image of the absolute conic. We now describe the procedure in grater detail.

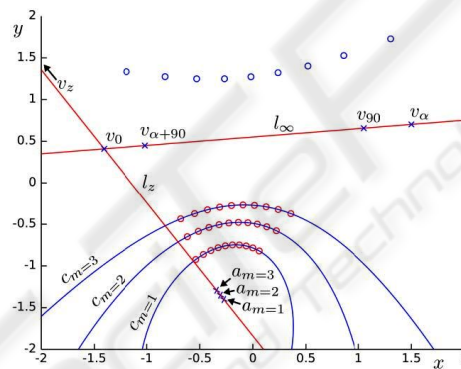


**Fig. 3.** The three conics allow us to derive a number of vanishing points, from which the camera intrinsic parameters can be computed.

At first, we compute the intersection points of the three conics. The only two common intersection points are the projections of the two circular points of the  $xy$  plane; they define the line at the infinity  $l_\infty$  of the  $xy$  plane in the image (horizon).

Let  $A_{m=x}$  be the center of  $C_{m=x}$ , and  $a_{m=x}$  its projection.  $a_{m=1}$  ( $a_{m=2}$ ,  $a_{m=3}$ ) is easily found as the pole of  $l_\infty$  with respect to  $c_{m=1}$  ( $c_{m=2}$ ,  $c_{m=3}$ ).

Let  $l_z$  be the projection of the  $F_z$  axis in the image. Since  $A_{m=1}$ ,  $A_{m=2}$  and  $A_{m=3}$  are aligned and lying on  $F_z$ ,  $l_z$  is determined as the line passing through the  $a_{m=x}$  points.

We name  $v_0$  the intersection of  $l_z$  with  $l_\infty$ , representing the horizontal vanishing point associated to a direction belonging to the symmetry plane which is defined by the camera center and rangefinder rotation axis. A vanishing point  $v_{90}$  perpendicular to such symmetry plane is found as the pole of  $l_z$  with respect to any of the  $c_{m=x}$  conics.

Let  $v_\alpha$  be a different vanishing point randomly chosen on  $l_\infty$ ; the vanishing point  $v_{\alpha+90}$  is found as the intersection of  $l_\infty$  with the polar line of  $v_\alpha$  with respect to any of the  $C_{m=x}$  conics.  $v_{\alpha+90}$  represents a direction parallel to the  $xy$  plane and perpendicular to the direction associated to  $v_\alpha$ .

Let  $v_z$  be the vanishing point representing the  $F_z$  direction.  $v_z$  lies on  $l_z$ ; its exact position can be recovered by considering points  $a_{m=1}$ ,  $a_{m=2}$  and  $a_{m=3}$ , which are projections of equidistant points on  $F_z$ ; by means of the cross-ratio invariance,  $v_z$  is easily determined.

In order to find the camera intrinsic parameters, we exploit the image  $\omega$  of the absolute conic [5, 2].  $\omega$  can be recovered by exploiting orthogonality relations between couples of the five vanishing points  $v_0$ ,  $v_{90}$ ,  $v_\alpha$ ,  $v_{90+\alpha}$  and  $v_\alpha$ , which translate to four linear equations:  $v_\alpha^T \omega v_{\alpha+90} = 0$ ;  $v_z^T \omega v_0 = 0$ ;  $v_0^T \omega v_{90} = 0$ ; and  $v_{90}^T \omega v_z = 0$

Once  $\omega$  is known, the matrix  $K$  containing the camera intrinsic parameters can be found using the Cholesky decomposition since  $\omega = K^{-T} K^{-1}$ .

### 3.4 Recovering the Rangefinder Parameters

**Computing  $\eta$ .** The  $\eta$  angle between rangefinder rays and the rotation axis  $F_z$  is easily recovered as the angle between the direction associated to a point  $p_{i,m=\infty}$  (which represents a vanishing point of a rangefinder ray direction) and the direction associated to  $v_z$ ; the angle between said directions can be computed since the camera intrinsic parameters are now known.

$p_{i,m=\infty}$  also allows us to recover the actual value of  $\phi_i$ , which was not previously known: in fact, the projection of  $R_i$ 's direction on the  $xy$  plane is identified by a vanishing point at the intersection between  $l_\infty$  and the join of  $p_{i,m=\infty}$  and  $v_z$ ; we can then measure  $\phi_i$  in relation to the direction identified by  $v_0$ .

**The Radius of Circles  $C_{m=x}$ .** In order to recover the remaining rangefinder parameters, we need to recover the radius of circles  $C_{m=x}$ .

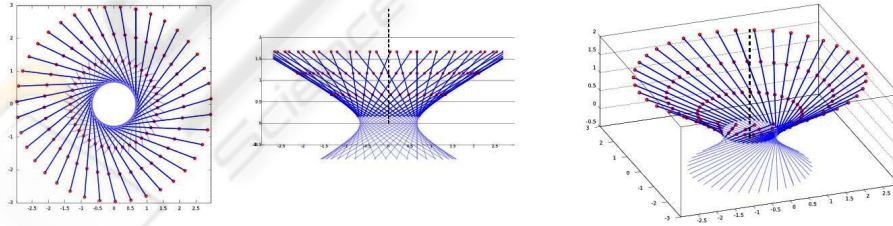


**Fig. 4.** The shape of the locus of rangefinder rays (a ruled quadric). The three circumferences  $C_{m=1}$ ,  $C_{m=2}$  and  $C_{m=3}$  are shown. Note that their radius varies along the  $F_z$  axis as an hyperbola.

We consider the two circles  $C_{m=1}$  and  $C_{m=2}$ , and the points  $P_{1,m=1}$ ,  $P_{1,m=2}$  lying on them, belonging to rangefinder ray  $R_1$ . Let  $\lambda$  be the radius of  $C_{m=1}$ : we are going to

recover  $\lambda$  by writing an equation involving the length of the projection on the  $xy$  plane of segment  $\overline{P_{1,m=1}P_{1,m=2}}$ .

Let  $\gamma_{m=1}$  be the (horizontal) direction of the radius  $\overline{A_{m=1}P_{1,m=1}}$ .  $\gamma_{m=1}$  is easily recovered as the direction associated to the vanishing point found at the intersection between  $l_\infty$  and the line on which said radius lies; the same holds for direction  $\gamma_{m=2}$  of the radius  $\overline{A_{m=2}P_{1,m=2}}$ .

Let  $\kappa$  be the ratio between radii  $\kappa\lambda = \overline{A_{m=2}P_{1,m=2}}$  and  $\lambda = \overline{A_{m=1}P_{1,m=1}}$ .  $\kappa$  can be recovered as follows: consider the image line bitangent to  $c_{m=1}$  and  $c_{m=2}$  at the same side w.r.t.  $l_z$ ; let  $a_z$  be the intersection point between said bitangent and  $l_z$ , and  $A_z$  its backprojection on  $F_z$ .  $\kappa$  is now found as the ratio between the lengths of segments  $\overline{A_zA_{m=2}}$  and  $\overline{A_zA_{m=1}}$ , which is computed exploiting the cross ratio invariance as:

$$\kappa = 2 \cdot \frac{\overline{a_z a_{m=2}} \cdot \overline{a_{m=0} a_{m=1}}}{\overline{a_z a_{m=1}} \cdot \overline{a_{m=0} a_{m=2}}}. \quad (2)$$

We finally get a single equation in the single unknown  $\lambda$ , which leads to:

$$\lambda = \cos(\eta) / \left\| \frac{\kappa \cos(\gamma_{m=1}) - \cos(\gamma_{m=2})}{\kappa \sin(\gamma_{m=1}) - \sin(\gamma_{m=2})} \right\|. \quad (3)$$

Once  $\lambda$  is known, the radii of  $C_{m=2}$  and  $C_{m=3}$  are easily found.

**Computing  $d_0$  and  $d_r$ .** We can now consider the function  $y = f(x)$  relating a rangefinder measure  $x$  to the radius of  $C_{m=x}$ : it is a hyperbola with vertical axis, and asymptotes forming an angle  $\eta$  with the  $x$  axis. Since we also have three points, we can identify the hyperbola. Its vertex'  $x$  and  $y$  coordinates are the rangefinder parameters  $-d_0$  and  $d_r$ , respectively. Alternatively,  $d_r$  can be recovered as the distance between the 3D line overlapping  $F_z$  and the measuring ray which is easily identified by using the data computed so far.  $d_0$  immediately follows.

This concludes the calibration of the rangefinder parameters.

### 3.5 Recovering the Camera Position and Rotation

Recovering the camera position and rotation in the reference frame  $F$  is now possible. The camera rotation matrix is easily computed from the location of vanishing points  $v_z$  and  $v_0$ . In order to compute the camera position, we can exploit the image of one of the diameters of  $C_{m=1}$ , whose 3D coordinates are now known.

## 4 Extensions, Discussion and Practical Issues

### 4.1 Degenerate Cases

If the camera center lies on the  $F_z$  axis, the centers of all circumferences  $C_{m=x}$  project to the same image point; therefore, the presented technique does not apply.

Another degenerate case happens if  $\eta = 0$  deg: then, the described procedure does not allow the camera intrinsic parameters to be calibrated. Still, the first steps of our

technique still allow us to recover a set of concentric, coplanar circles: by gathering a first complete set of observations followed by another set acquired with a different camera pose, the camera parameters can be calibrated and the rest of the procedure follows with trivial modifications.

#### 4.2 Exploiting Additional Observations

Since data gathering is such an easy and practical task, many additional observations may be available in most scenarios with little additional effort. Our technique is easily adapted to exploiting them, in order to improve the results accuracy and robustness to noise.

For each of the  $\phi_i$  angles, we require at least three observations in order to recover  $p_{i,m=x}$  points by exploiting cross ratio invariance. If more than three different observations for a given  $\phi_i$  angle are available, the cross ratio can be estimated robustly to noise. Note that measurement errors originate both from noise on the rangefinder readings, and from uncertainty in the laser dot localization in the image.

If at least three observations are provided for more than five different  $\phi$  angles, each of the additional angles provides one extra point for estimating  $c_{m=x}$  conics, which improves noise resilience as well; then, known conic fitting techniques [3] can be applied. Each of the  $p_{i,m=x}$  points may be weighted differently, based on its confidence.

#### 4.3 Exploiting a Priori Knowledge

In many scenarios, some of the system parameters may be known *a priori*; then, our technique can be adapted in order to exploit this knowledge, in order to improve noise resilience. Some common scenarios follow:

$d_r = 0$  : in this case, the surface defined by the rangefinder rays is a cone: the last part of the calibration can therefore be skipped; in fact, once  $\lambda$  is computed,  $d_0$  is immediately found.

**Rangefinder parameters known:** if all the rangefinder parameters are known a priori and the  $\phi$  angle of each observation is calibrated, rangefinder rays and laser dot coordinates can be localized in reference frame  $F$ . Camera calibration then reduces to the well-studied scenario in which all of the observed points have a known 3D position.

**Camera intrinsic parameters known** : in this case, the first steps of the technique can be skipped.

#### 4.4 Visibility and Localization of the Laser Dot

Localizing the laser dot in an image is a task which is easily made automatic even in lit environment: a simple solution, also suggested in [7] is shooting two images, one with the laser on and one with the laser off; the difference image between the two then isolates the laser dot, whose exact coordinates can be taken either by first binarizing the image then using the skeletonize morphological operator, or by computing the barycenter of the spot.



In order to localize the dot, an obvious prerequisite is that it is actually visible in the image: this may be a problem when using a laser working in the near-infrared wavelengths, whose dots will therefore irradiate light outside the visible part of the electromagnetic spectrum: although image sensors are very sensible to such wavelengths, sometimes cameras use filters to minimize their effect, which should be removed.

## 5 Experimental Results and Implementation Notes

First, the technique has been validated by implementing a matlab-based simulator of the camera-rangefinder system, also accounting for a customizable amount of normally-distributed noise affecting both the image coordinates of the laser dot projection and the readings of the rangefinder; we also developed a matlab implementation of the calibration technique. When operating on clean data, the procedure yields results perfectly adhering to ground truth (up to negligible errors due to numerical precision issues); this validates the soundness of our approach. Figures 1 (right), 2 and 3 are related to such experiments, with the following parameters:  $d_0 = 2$ ,  $d_r = 1$ ,  $\eta = \pi/8$ , and a natural camera with the principal point at the center of the image plane and focal length 0.55 times the image width. When adding noise, the quality of results drops rather dramatically, due to the geometrical nature of the technique which is not resilient to noise. In particular, intersecting conics returns unreliable circular points. Implementing the techniques introduced in Section 4.2 allows to exploit additional observations, thus improving noise resilience.

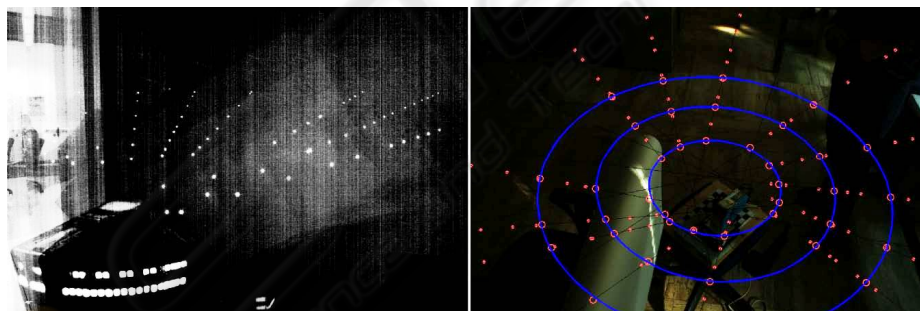


**Fig. 5.** Left: addition of many images shot in a dark room: the laser dots and their alignment are visible; the dataset associates a range measurement with each. Right: part of the construction in another real setting, on the background of one of the 92 images comprising the dataset; observations (red dots) and fitted lines (black); computed image points corresponding to 200mm, 400mm and 600mm measures (red circles); fitted conics (blue ellipses);  $l_\infty$  is over the top of the image. Note significant span of  $\phi$  angles, which enables a much improved conic fitting.

We also applied the technique to camera images, acquired in two different sets with different parameters, composed by 77 and 92 observations, respectively. Due to noise in the image and rangefinder readings, all the observations must be exploited in order to complete the calibration procedure correctly. However, we identified that some steps of

the technique, such as the intersection of conics for finding  $l_\infty$ , are acting as bottlenecks and being severely affected by noise. Such steps of the algorithm are currently being improved and substituted with noise-resilient implementations in order to improve calibration accuracy in presence of noise.

## 6 Conclusions and Future Works

We developed a geometrical technique for mutually calibrating a camera and a laser rangefinder. The technique is attractive because of its generality, and because it does not assume anything about the environment; the data collection step is also extremely simple and straightforward.

We validated the technique by using both real and simulated data: the results confirm the correctness of the approach, but also highlight the expected weakness to noise in the data when using the minimal amount of observations. In order to be practical in real scenarios, we described a number of possible improvements aimed at increasing robustness to noise; in particular, since data collection is fast and simple, the process can be automated and may gather a large amount of observations.

We are currently implementing modifications to the technique in order to maximally exploit all available data, and replacing steps heavily affected by noise with noise-resilient alternatives. Moreover, we are planning an extension for the mutual calibration of a camera and a SICK laser rangefinder, whose scans are visible in the images as jagged lines.

## References

1. M. Antone and Y. Friedman. Fully automated laser range calibration. In *Proc. of BMVC 2007*.
2. Carlo Colombo, Dario Comanducci, and Alberto Del Bimbo. Camera calibration with two arbitrary coaxial circles. In *Proc. of ECCV 2006*.
3. Andrew W. Fitzgibbon and Robert B. Fisher. A buyer's guide to conic fitting. In *Proceedings of BMVC 1995*.
4. Pierre Gurdjos, Peter Sturm, and Yihong Wu. Euclidean structure from  $n \geq 2$  parallel circles: Theory and algorithms. In *Proc. of ECCV 2006*.
5. R. I. Hartley and A. Zisserman. *Multiple View Geometry in Computer Vision*. 2004.
6. G. Jiang, H. Tsui, L. Quan, and A. Zisserman. Geometry of single axis motions using conic fitting. 2003.
7. C. Mei and P. Rives. Calibration between a central catadioptric camera and a laser range finder for robotic applications. In *Proc. of ICRA 2006*.
8. Tomáš Svoboda, Daniel Martinec, and Tomáš Pajdla. A convenient multi-camera self-calibration for virtual environments. *PRESENCE: Teleoperators and Virtual Environments*.
9. Qilong Zhang and R. Pless. Extrinsic calibration of a camera and laser range finder (improves camera calibration). In *Proc. of IROS 2004*.